Volume 9, Issue 5, 2019, 4205 - 4216 ISSN 2069-5837
Biointerface Research in Applied Chemistry
www.BiointerfaceResearch.com
https://doi.org/10.33263/BRIAC95.205216
Original Review Article Open Access Journal
Received: 12.08.2019 / Revised: 24.08.2019 / Accepted: 25.08.2019 / Published on-line: 26.08.2019

A review on giant piezoelectric coefficient, materials and applications

Singampalli Ramesh[1], Dachepalli Ravinder[2], Kadiyala Chandra Babu Naidu[1,*], Nagasamudram Suresh Kumar[3], Kurapati Srinivas[1], D. Baba Basha[4], B. Chandra Sekhar[5]

[1]Department of Physics, GITAM Deemed to be University, Bangalore-562163, India
[2]Department of Physics, Osmania University, Hyderabad, 500007, Telangana. India
[3]Department of Physics, JNTUA, Anantapuramu-515002, A.P, India.
[4]College of Computer and Information Sciences, Majmaah University Al'Majmaah, K.S.A-11952.
[5]Vignan's Institute of Engineering for Women, Visakhapatnam, India

*corresponding author e-mail address:*chandrababu954@gmail.com* | Scopus ID: 56520309700 |

ABSTRACT
The current work deals with the review of various piezoelectric materials and their piezoelectric coefficient (d_{33}) for probable piezoelectric device applications. In addition, the comprehensive analysis of the data of d_{33} obtained for distinct compounds is also made. Furthermore, the best suited material compositions are highlighted.

Keywords: *Electroceramics; Sensors, Piezoelectrics; PZT; Ferroelectrics.*

1. INTRODUCTION

It has been a well known fact that the piezoelectric materials play a major role in electronic devices such as sensors, accelerators, ultrasonic motors, transducers, actuators, filters and resonators, and micro electromechanical systems (MEMS). Piezoelectric ceramics were used for scientific interest (industrial applications) around 1950 [1].Among all the electroceramics, the piezoelectric ceramics were special due to their characteristics. These materials are actively used because of their environmental friendly substances.

Piezoelectricity is in general the accumulation of charges on the surface of solid material when the material is subjected to the mechanical stress[1]. Herein, the solid materials such as crystalline solids, ceramic materials, parts of the organic matter viz., bones, DNA, proteins etc., can be considered into the account of piezoelectric materials[1]. The piezoelectric materials exhibit several potential applications towards the progress of scientific community. In view of this, different applications were noticed in distinct industries like computer, automotive, medical, military, consumer etc [2]. Specifically, these are of high performance multilayer piezoelectric actuators (MPAs), ultrasonic transducers, communication circuit components, sensors, accelerators, filters, resonators, ultrasonic motors, energy harvesters, micro-electromechanical systems (MEMSs) etc [2-5]. These applications are mainly dependent on various piezoelectric characteristics such as electromechanical communication (K_p), relative dielectric permeability ($\varepsilon^T_{33}/\varepsilon_o$), specific volume electric resistance (ρv), density (ρ), water absorption (W), piezo-modules in a dynamic mode (d_{31}, d_{33}), piezo-modules in a static mode (d_{31}), young's modulus (Y^Y_{31}), speed of sound (υ^j_i), good mechanical quality (Q_M), relative frequency deviation in the range of working temperatures from the frequency measured at the adjustment temperature ($\delta_\Theta f/f_r$), corner of dielectric loss tangent in weak electric fields (tg δ), electrical durability (E_{np}), Curie temperature (T_c), mechanical durability limit with static compression (σ_{compre}), mechanical durability limit with static bending (σ_b), mechanical durability limit with static stretching (σ_s) [6]. As a result of these characteristics, the piezoelectric materials showed the above stated applications. However, it was an observed fact that several scientists put forth on the synthesis of the giant piezoelectric materials containing giant d_{33} coefficient [7-9]. In this context, the authors intended to review the giant piezoelectric specimen and further to elucidate the piezoelectric parameters of the corresponding samples.

1.1 Theory.

It is a well known fact that the piezoelectric effect can be normally obtained as a result of the interaction between mechanical deformation and the applied input electric field. However, the piezoelectric coefficient is a significant parameter in order to study the piezoelectric properties as well. Let the mechanical stress and the electric charge density be designated by T_{jk}& D_i respectively. In case of piezoelectricity, the linear relationship can be found between T_{jk}& D_i. This can be referred as direct piezoelectric effect and is mathematically given by $D_i. = d_{ijk} . T_{jk}$ [10], herein T_{jk} refers to the stress tensor of 2nd rank, and d_{ijk} is called as piezoelectric coefficient (C/N) of 3rd rank. Moreover, the converse of piezoelectric effect also becomes true. According to this converse effect (mechanical deformation of piezoelectric crystal under the external electric field), the mathematical expression can be given by: $x_{jk} = d_{ijk}^T .E_i$, where the x_{jk} refers to the strain of 2nd rank, E_i is associated to the input electric field, and d_{ijk} is assigned to the parameter of converse piezoelectric coefficient (m/V). In addition, the superscript T indicates the transposition of the matrix. However, as per the thermo-dynamical illustrations [10], the piezoelectric coefficients in direct and converse reactions become identical. It is also indicated that the strain and stress are the symmetrical tensors and therefore the relationship between the two types of piezoelectric coefficients is given bydijk=dikj. In matrix form, the direct and converse piezoelectric effects can be given by

$$\begin{pmatrix} D1 \\ D2 \\ D3 \end{pmatrix} = \begin{pmatrix} 0 & 0 & 0 & 0 & d15 & 0 \\ 0 & 0 & 0 & d24 & 0 & 0 \\ d31 & d32 & d33 & 0 & 0 & 0 \end{pmatrix} \begin{pmatrix} T1 \\ T2 \\ T3 \\ T4 \\ T5 \\ T6 \end{pmatrix} \& \begin{pmatrix} S1 \\ S2 \\ S3 \\ S4 \\ S5 \\ S6 \end{pmatrix} = \begin{pmatrix} 0 & 0 & d31 \\ 0 & 0 & d32 \\ 0 & 0 & d33 \\ 0 & d24 & 0 \\ d15 & 0 & 0 \\ 0 & 0 & 0 \end{pmatrix} \begin{pmatrix} E1 \\ E2 \\ E3 \end{pmatrix}$$

Experimentally, the piezoelectric coefficient can be measured and the method is as follows: The desired sample is kept in the sample holder. Further, the direct current voltage is applied with the help of an electrode. Later on, the deformation takes place and meanwhile, it should be measured in the similar direction of the deformation. In next step, one can measure the longitudinal piezoelectric coefficient which is designated by d_{zz}. Herein, the two subscripts sequentially reveal the direction of deformation as well as the applied input electric field. The d_{zz} parameter can be represented in the tetragonal symmetry group (0.4 cm) as follows [10-11]: $d_{zz} = (d_{31} + d_{15}) \text{Sin}^2\theta \text{ Cos}\theta + d_{33} \text{ Cos}^3\theta$, where θ is the angle between (001) piezoelectric crystal axis & measurement direction. But, in the present mentioned experiment, the direction of (001) crystal axis is perpendicular to the sample. That is, the θ becomes equal to zero. Hence, the d_{zz} and d_{33} become equal.

In general, the trend of produced strain versus the electric field plot shows a butterfly loop model (Fig.1a & b). Herein, the deformation of crystal takes place in linear direction to the applied field. In addition, the formed butterfly shape is also acquired owing to the three effects. These are (i) converse piezoelectric effect, (ii) switching of domain walls, and (iii) movement of domain walls. If the input field tends to zero, the strain also becomes zero as shown in Fig.1a (at point a). Further, the electric field is increased (a-c); the deformation in crystal also increases linearly. As the input field is decreased (c-d), the polarization is altered by 180^{o}C at the coercive field (at d). Once the switching is over, the polarization becomes in the parallel direction of the electric field. Therefore, the strain approaches to positive value as shown at e. As a result, further the strain follows a linear manner against the input field. As a whole, it shows a loop. Furthermore, the piezoelectric coefficient can be calculated using the slope of the linear portion of the loop.

1.2 Experimental set up to find piezoelectric coefficient (d_{33}).

It is an established fact that the d_{33} value is a dependent parameter of relative permittivity and remanent polarization (P). According to Landau-Ginsburg-Devonshire (LGD), it is mathematically given by: $d_{33} = 2Q_{11}\varepsilon_o\varepsilon_{33}P$, herein Q_{11} shows the electrosrtictive constant of the paraelectric phase. Commonly, this value changes from 0.05 - 0.1 m^4/C^2 for various samples. The ε_o & ε_{33} are the permittivity of free space & permittivity of samples respectively and P reveals the remanent polarization [2]. However, the d_{33} value can be enhanced by optimizing the ε_{33}& P. This can be achieved by means of doping element and further controlling the microstructure. In fact, the microstructure as well as transport properties can be well controlled by means of grain orientation even in the case of absence of doping element. This will not affect the phase transition temperatures (T_c) [3, 4].

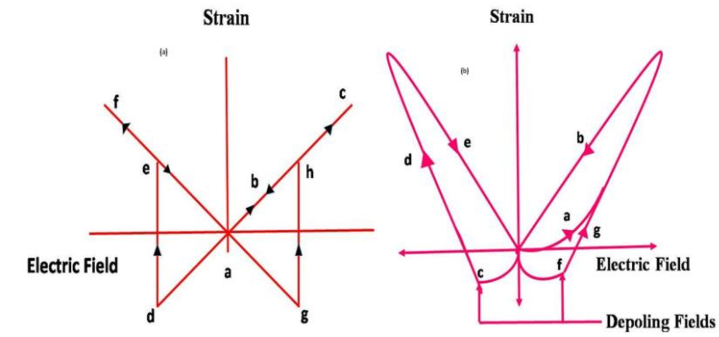

Figure 1.(a) the ideal loop of the strain versus the electric field; (b) the actual butterfly loop.

Figure 2. Photograph of d_{33} experimental set up (Bulletin de la SociétéMinérologique de France. 3(1880) 90–93).

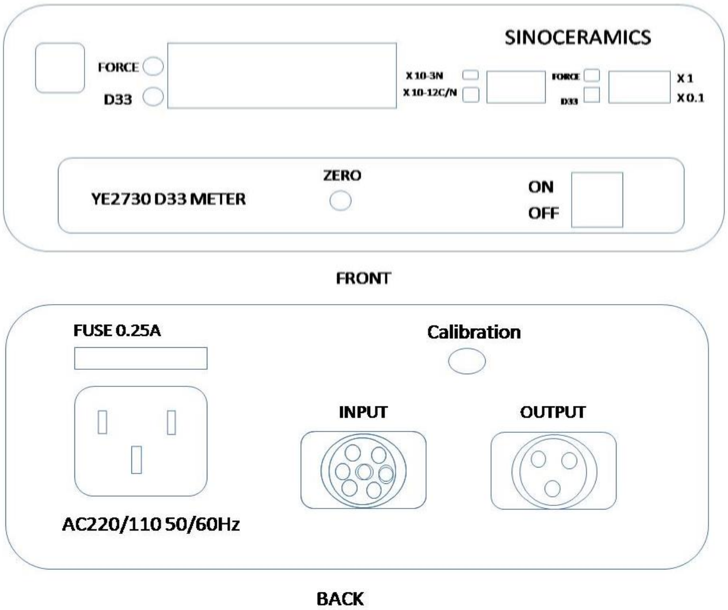

Figure 3. Front and back schematic diagrams of d_{33} experimental set up.

The piezometer (Fig.2) includes a sample holder in which the sample in the form of ceramics, polymers and thin films. Inthe beginning, the system needs to be calibrated using a reference sample of known d_{33} value. Further, it is subjected to low frequency force. As a result, the electrical signals will be processed from the material and subsequently, it provides the direct reading of d_{33} parameter. This is a significant parameter in order to evaluate the efficiency of piezoelectric material.

Specifically, this implies the charge per unit force in the direction of polarization. Usually, this is said to be Berlincourt method. The advantage of this system is to get the d_{33} value with low input frequency and quick in time. At present, this is the easiest system in order to obtain d_{33} value. Besides, many advanced methods provide excellent resolution, consistency etc., to any kind of sample. The schematic representation of various front & back components in the piezometer is shown in Fig.3. Similarly, the schematic experimental set up is shown in Fig.4. It includes the bottom and top probes which contain a gap. In the gap the desired sample is inserted to find d_{33}. The adjustment provision is also accommodated.

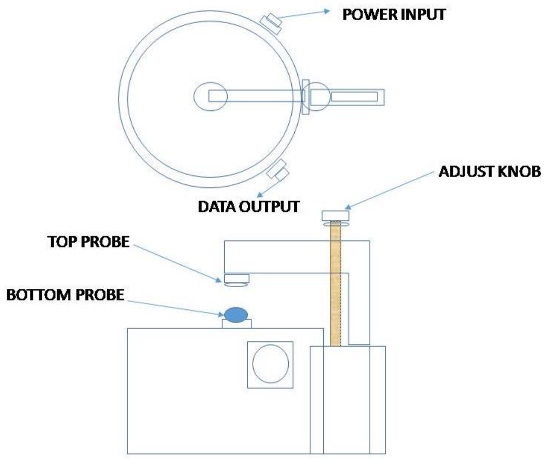

Figure 4. Schematic diagram of d_{33} experimental set up.

2REVIEW ON D_{33} COEFFICIENT AND PIEZOELECTRIC MATERIALS

2.1 Barium Titanate Based Materials (BTX).

It was a reported fact that the piezoelectric materials like barium titanate and its based materials (ceramics & thin films) exhibited extensive applications as actuators, sensors, transducers etc.[12-17]. In general, sensors will have the capacity to obtain mechanical energy from I/P energy. This I/P energy can be either in the form of electrical, electrostatic or thermal energy. In addition, the piezoelectric actuators need the efficiency of piezoelectric parameters such as the maximum strain output, strain, maximum resonance speed, electric charge distribution and the maximum displacement control accuracy [12]. Due to the huge electromechanical response of piezoelectric specimen, they acquired good attention in highly sophisticated equipments like atomic force microscopy and scanning tunneling microscopy. As a whole, it was noticed that the larger is the electromechanical response, the higher is the performance of piezoelectric actuators. This kind of behavior can be attributed to the high numerical values of longitudinal electromechanical coupling factor (k_{33}) and longitudinal piezoelectric coefficient (d_{33}) [12, 13]. Based on these two parameters, one can justify whether the piezoelectric specimen is well suited for the high performance actuator device applications or not [14]. In view of this, many researchers performed extensive investigations on distinct piezoelectric materials. However, in the present review work, we highlighted the piezoelectric materials according to the parent and its based materials. The major role of d_{33} parameter in ensuring the piezoelectric efficiency was done at length and different values were reported in Table.1.

From Table.1, it can be noted that the piezoelectric constant (d_{33}) was varying from 4 to 620 pC/N for barium titanate (BT) and BT based materials. These values were achieved as a result of various synthesis approaches to prepare the materials. Besides, the transition temperature (T_c) of BT was observed to be changing from 120 to 130^{o}C depending upon the synthesis method. It was also evident from Table.1 that the huge d_{33} value ~ 416 pC/N was found for BT material (prepared through spark plasma sintering) with 100 nm domain size. In the same fashion, the spark plasma sintered (SPS) BT of domain size 500 nm revealed d_{33} ~ 216 pC/N. Likewise, interestingly, the BT sample with domain size of 100 nm which was prepared by hydrothermal synthesis and normal sintering (NS) showed a d_{33} value about 193 pC/N. This established a fact that the kind of sintering process can independently alter the piezoelectric efficiency of samples. During the SPS process the BT attained the tetragonal phases (JCPDS: 05-0626) while the NS method reinforced to obtain the cubic BT phases. This confirmed us that the presence of tetragonal phases in BT allowed getting high d_{33} value. On the other hand, the domain size factor influenced in achieving the high/low d_{33} value. Shao et al.[18] and Sharma et al.[13] reported that the nano-domain size is the dominant factor in order to enhance the piezoelectric properties of materials. That is, for small sized domains, one can expect high d_{33}, while the small value of d_{33} can be observed for the materials possessing large domain size. Using the conventional solid state reaction (SSR) method almost identical d_{33} values were noted around 190-200 pC/N [13, 18]. But the BT single crystal (grown using Bridgeman technique) exhibited d_{33} ~ 86 pC/N which is very small in magnitude when compared with d_{33} of BT prepared by NS & SPS methods. This manifested that the polycrystalline BT material expressed some what high d_{33} while single crystal BT showed moderate value of d_{33}. Due to the high d_{33} value of BT, it showed many applications like charge stored capacitors, piezoelectric transducers, and actuators [13, 18].

Further, the BT based ceramics, alloys and composites (as shown in Table.1) [19-35] also expressed the d_{33} value changing from 4 to 620 pC/N. Among these materials, $Ba(Zr_{0.2}Ti_{0.8})TO_3$-50$(Ba_{0.7}Ca_{0.3})TiO_3$ (620 pC/N), BT-x(CT-BS) (570 pC/N) and $Ba(Ti_{0.88}Sn_{0.12})O_3-30(Ba_{0.7}Ca_{0.3})TiO_3$ (530 pC/N) showed the highest value of d_{33} reported till now using BT based materials. In particular, the $Ba(Zr_{0.2}Ti_{0.8})TO_3$-50$(Ba_{0.7}Ca_{0.3})TiO_3$ revealed the highest d_{33} value of 620 pC/N. It was understood that the BT material when mixed with the elements like Zr & Ca performed high piezoelectric coefficient. The reason was due to the presence of three phase structure as reported in the literature[7]. Herein, the three phase structure is related to the rhombohedral-orthorhombic-tetragonal (R-T-O). As a whole, this R-T-O phase structure is responsible for high d_{33}. This was occurred in the case of BT-x(CT-BS) also at x = 0.16 owing to the same reason [7]. However, these types of BT based materials exhibited the applications as well in electromechanical actuators, MEMS, NVRAM, capacitors, and sonar sensors [5-10].

2.2 Lead Titanate Based Materials (PTX).

The $PbTiO_3$ (PT) prepared via different synthesis methods acquired the d_{33} value ranging from 56 to79 pC/N [36-38]. This was five times smaller than the d_{33} of BT material. The presence of tetragonal phases may be responsible for this. However, the PT also shows the tetragonal structure. The grain size and synthesis method can also become a reason for this kind of difference. Therefore, several dopants and substitutions were made to the PT material in order to achieve high d_{33}. The different d_{33} values of different PT based materials were reported in Table.2.

It was noticed that the PT based materials in the form of composites, thin films etc., attained the d_{33} values altering from 10 to 3500 pC/N [36-61]. The sol-gel processed PZT thin film showed a small piezoelectric coefficient about 10 pC/N. Specifically, the single crystal PT based materials attributed to the high d_{33} value. This was obtained owing to the existed high strains achieved for <001> oriented rhombohedral crystals [45]. In view of this, the highest value of d_{33} ~ 3500 pC/N for (1-x)[$Pb(Mg_{1/3}Nb_{2/3})O_3$]-x[$PbTiO_3$] (PMN-PT) prepared via Bridgeman technique. In addition, some more single crystals were found with high piezoelectric response like $Pb(Mg_{1/3Nb2/3})O_3$–$PbZrO_3$–$PbTiO_3$ (PMN–PZT)-S-Crystal, PZN-8%PT crystal orientation <001> [$Pb(Zn_{1/3}Nb_{2/3})O_3$–$PbTiO_3Pb(Zn_{1/3}Nb_{2/3})O_3$–$PbTiO_3$], PZN, crystal orientation <001> etc. Therefore, it was confirmed that the crystal orientation plays a vital role in acquiring the high d_{33} value. The corresponding transition temperatures were also noted in Table.2. Thus, these materials were extensively used for variety of applications such as data memory, storage, energy harvesting, solar energy conversion, and high power transducers. The T_c values of various samples were also noted in Table 2.

Table 1. Data on BT and its based materials.

BT based materials	d_{33} (pC/N)	T_c (°C)	Synthesis Method	Applications	Ref.
$BaTiO_3$	200	120	conventional method (SSR)	capacitors, piezoelectric transducers	[19]
$BaTiO_3$ (BT-100-SPS)	416	120	Spark plasma sintering (SPS)	capacitors, piezoelectric transducers	[20]
$BaTiO_3$ (BT-100-NS)	193	120	hydrothermal synthesis	capacitors, piezoelectric transducers	[20]
$BaTiO_3$ (BT-500-SPS)	216	120	spark plasma sintering (SPS)	capacitors, piezoelectric transducers	[20]
$BaTiO_3$	191	130	conventional method (SSR)	Actuator	[21]
$BaTiO_3$ single crystal	86	130	Bridgeman Technique	Actuator	[21]
Barium Titanate and nano-akermanite, (BT/nAK) BT90/nAK10	4		freeze-casting technique		[22]
$0.95BaTiO_3$-$0.05CaTiO_3$-Co	150	105			[23]
$0.9BaTiO_3$-(0.1-x)$CaTiO_3$-x$BaSnO_3$ [BCT-xBS]	469 - 1335		SSR		[24]
$Ba(Ti_{0.88}Sn_{0.12})O_3-30(Ba_{0.7}Ca_{0.3})TiO_3$	530		SSR	electromechanical actuator applications	[25]
$Ba(Zr_{0.2}Ti_{0.8})TO_3$-50$(Ba_{0.7}Ca_{0.3})TiO_3$	620		SSR	electromechanical actuator applications	[25]
$(Ba_{0.98}Ca_{0.02})(Ti_{0.96}Sn_{0.04})O_3$	510		SSR	electromechanical actuator applications	[25]
$(Ba_{0.97}Ca_{0.03})(Ti_{0.94}Sn_{0.06})O_3$	440		SSR	electromechanical actuator applications	[25]
BT-x(CT-BS)	570		SSR	electromechanical actuator applications	[25]
$(Ba_{0.93}Ca_{0.07})(Ti_{0.95}Zr_{0.05})O_3$	387	108	SSR		[26]
$(Ba_{1-x}Ca_x)(Ti_{0.98}Zr_{0.02})O_3$	375	115	SSR		[27]
x$(Na_{0.5}Bi_{0.5})TiO_3$-y$(K_{0.5}Bi_{0.5})TiO_3$-z$BaTiO_3$ (x þ y þ z¼ 1; y:z¼ 2:1)	145	302			[23]
BC5 ($Ba_{0.9}Sr_{0.1}Zr_{0.1}Ti_{0.9}O_3$-$CoFe_2O_4$)	281		Mechanochemical activation method.	MEMS, NVRAM, capacitors, actuators, sonar sensors	[28]
$0.94Na_{0.5}Bi_{0.5}TiO_3$-$0.06BaTiO_3$	102.6		sol-gel method		[29]
$Ba_{0.98}Ca_{0.02}TiO_3$	290		SSR	sensors, actuators, fuel injectors & transducers	[30]
$(Ba_{0.85}Ca_{0.15})(Zr_{0.1}Ti_{0.9})O_3$(BCZT)	486	90	SSR	actuators, ultrasonic transducers,	[31]

				energy harvesters , smart sensors	
$Ba_{0.90}Ca_{0.10}Ti_{0.90}Sn_{0.10}O_{3-x}Y_2O_3$ (BCTSY)	650		SSR		[32]
(1-x)$Ba(Zr_{0.2}Ti_{0.8})O_3$–x$(Ba_{0.7}Ca_{0.3})TiO_3$	464	420	SSR	energy harvesting application	[33]
$(Ba_{0.85}Ca_{0.15})(Zr_{0.1}Ti_{0.9})O_3$	600				[34]
$(Ba_{0.85}Ca_{0.15})(Zr_{0.10}Ti_{0.90})O_3$–*x*$LiTaO_3$	433	102	SSR	actuators, sensors, transducers	[35]

Table 2. Data on PT and its based materials.

PT based materials	d_{33} (pC/N)	T_c (^oC)	Synthesis Method	Applications	Ref.
$PbTiO_3$	56	475	tartrate precursor method		[36]
$PbTiO_3$	79				[37]
$PbTiO_3$ (at 750^{o}C calcined temp)	75		tartrate precursor method		[38]
(1-x)[$Pb(Mg_{1/3}Nb_{2/3})O_3$]-x[$PbTiO_3$] (PMN-PT)	~3500		Bridgman technique		[39]
1-x)[$Pb(Mg_{1/3}Nb_{2/3})O_3$]-x[$PbTiO_3$] (PMN-38PT)	300-1200				[40]
PZT thin films	10		sol-gel processing		[41]
Cellulose paper derived ceramics (CPDC)	50				[42]
PZT60/40films.	100				[43]
$Pb(Mg_{1/3}Nb_{2/3})O_3$–$PbZrO_3$–$PbTiO_3$ (PMN–PZT)-R – Ceramic	230				[44]
$Pb(Mg_{1/3}Nb_{2/3})O_3$–$PbZrO_3$–$PbTiO_3$ (PMN–PZT)-T-Ceramic	1100				[44]
$Pb(Mg_{1/3}Nb_{2/3})O_3$–$PbZrO_3$–$PbTiO_3$ (PMN–PZT)-S-Crystal	1530				[44]
PZN-8%PT crystal orientation <001> $Pb(Zn_{1/3}Nb_{2/3})O_3$–$PbTiO_3$$Pb(Zn_{1/3}Nb_{2/3})O_3$–$PbTiO_3$	2500		high temperature flux technique	solid state actuators	[45]
PZN, crystal orientation <001>	1100		high temperature flux technique		[45]
PZN, crystal orientation <111>	83		high temperature flux technique		[45]
PZN-8%PT, crystal orientation <111>	84		high temperature flux technique		[45]
PZT	750		high temperature flux technique		[45]
$Pb(B_1,B_2)O_3$-PT	1500		high temperature flux technique		[45]
PZN-PT	1600		high temperature flux technique		[45]
PZN direction <111>	83		high temperature flux technique		[45]
PZN-8%PT	84		high temperature flux technique		[45]
PZN along <001>	1100		high temperature flux technique		[45]
PZN-8%PT along <001>	2500		high temperature flux technique		[45]
0.955$Pb(Zn_{1/3}Nb_{2/3})O_3$–0.045$PbTiO_3$ along <001>	2280		grown using the hightemperature flux technique.		[46]
0.955$Pb(Zn_{1/3}Nb_{2/3})O_3$–0.045$PbTiO_3$<111>	92				[46]
PZT ceramics	219.4				[47]
lead zirconatetitanate (PZT) thinfilms	12		sol-gel technique		[48]
PZT Fe	230		SSR		[49]
PZT Nb	470		SSR		[49]
PZ26	290	330			[50]
PZ27	425	350			[50]
PZT5A4	460	360			[50]
PZT507	820	165			[50]
PLZT	108				[51]
PZT-5A	3.74				[52]
PZT-5H	5.93				[52]
PZT-7A	1.53				[52]
0.67$Pb(Mg_{1/3}Nb_{2/3})O_3$– 0.33$PbTiO_3$	>1900				[53]
PZT-4D	246				[54]
PZT-5H	677				[54]
PZT(52/48)	135		tartrate precursor method		[36]
0-3 PZT	87				[36]
PZT(57/43)	200				[36]

PZT	75				[36]
La doped PZT	380				[36]
MPSZT0.5	270				[36]
$Pb(Zr_{0.52}Ti_{0.48})O_3$	223				[36]
$Pb_{0.9725}(Zr_{0.52}Ti_{0.48})_{0.945}Nb_{0.055}O_3$	386				[36]
PZT	505				[36]
PZT-2TZ	475				[36]
PZT-5TZ	395				[36]
PZT-10TZ	311				[36]
PZT4	225				[36]
PZT-5H	585				[36]
0.9PZT-0.1CFO	38				[36]
Nano $PbZr_{0.4}Ti_{0.6}O_3$	528				[36]
0.67PMN- 0.33PT	660		Molten salt method	Storage memories & energy harvesting, solar energy conversion	[55]
$Pb(In_{0.5}Nb_{0.5})O_3$-$Pb(Mg_{1/3}Nb_{2/3})O_3$-$PbTiO_3$:Mn single crystals	800-1960		Bridgman technique	high power transducer	[56]
PIMNT 8/59/33	500	187			[57]
PIMNT 8/59/33	510	197			[57]
PIMNT 24/42/34	505	219			[57]
PIMNT 32/33.5/34.5	495	239			[57]
PIMNT 40/25/35	430	258			[57]
PIMNT 48/16/36	430	279			[57]
PIMNT 56/8/36	440	300			[57]
PIMNT 63/0/37	435	320			[57]
PIMNT 23/41/36	550	231			[57]
PIMNT 23.5/41.5/35	515	223			[57]
PIMNT 24/42/34	505	219			[57]
IMNT 24.5/42.5/33	465	211			[57]
PIMNT 25/43/32	465	213			[57]
$(1-x)[(Pb_{1-y}Sr_y)(Mg_{1/3}Nb_{2/3})O_3]$-$x(Pb_{1-y}Sr_yTiO_3)$ (PsMN–PsT)	630	206	solution coating technique	actuator and biosensors	[58]
MnO_2-doped $Pb(Yb_{1/2}Nb_{1/2})O_3$-$Pb(Zr,Ti)O_3$	418	379	SSR	sensors, transducers & actuators	[59]
$0.49Pb(Ni_{1/3}Nb_{2/3})O_3$-$0.51Pb(Hf_{0.3}Ti_{0.7})O_3$ (PNN-PHT)	957		two-step precursor technique	transducer, sensor, buzzer & actuator,	[60]
$0.15Pb(Mg_{1/3}Nb_{2/3})O_3$-$0.38PbHfO_3$-$0.47PbTiO_3$ (PMN-PH-PT)	593	193	Citrate Method		[61]

2.3. Bismuth Titanate Based Materials (BITX).

It was also observed that the rhombohedral bismuth titanate and its based materials revealed the considerable piezoelectric response. Besides, the undoped BIT expressed the ferroelectric transition temperature at 670 ^oC [62]. In connection with d_{33}, it showed value of 40 pC/N. Comparatively, this was smaller than the d_{33} of BT & PT which suggested moderate piezoelectric efficiency. Therefore, it was expected for ferroelectric and piezoelectric device applications [63]. For further increase of d_{33} value, several additives were mixed to the BIT. As a result, few elements such as Sr, Na, Nd, K etc., were doped to BIT. The obtained d_{33} data werelisted in Table.3 [62-71]. It was clear from Table.3 that the d_{33} of BIT based samples was observed to be changing from 17 to 650 pC/N. In this case also, the maximum value of $d_{33}$of 650 pC/N was achieved for BNBT-5.5 single crystal [64]. For BT, and PT based materials also the similar observations were noted. Moreover, it was noticed that the single crystal piezoelectric materials depending upon the type of dopant/substituent, the piezoelectric coefficient was much improved. The T_c values of various samples were also noted in Table.3.

2.4. Sodium Niobate Based Materials (NNX).

The sodium niobate ($NaNbO_3$ (NN)) and its based materials revealed the piezoelectric coefficient ranging from 28 to 410 pC/N. It was observed that the undoped NN showed d_{33} ~ 28 pC/N. It is of small value in comparison with the BT, PT, & BIT. However, the potassium elements improved three times its d_{33} value. Latter, the different combinations were prepared using the solid state reaction method. The d_{33} values of those materials were listed in Table.4. It was found that the d_{33} was changing from 80 to 410 pC/N [72-78]. These materials showed data memory and storage, energy harvesting, solar energy conversion applications. The T_c values of various samples were also noted in Table.4.

Table 3. Data on BIT and its based materials.

BIT based materials	d_{33} (pC/N)	T_c (^oC)	Synthesis Method	Applications	Ref.
($Bi_4Ti_3O_{12}$, BIT)	40	670	polymeric precursor method	ferroelectric and piezoelectric devices	[62]
$SrBi_2Ta_2O_9$ films	17		polymeric precursor method	ferroelectric & piezoelectric devices	[62]

BIT based materials	d_{33} (pC/N)	T_c (^oC)	Synthesis Method	Applications	Ref.
Nd-doped $Bi_4Ti_3O_{12}$	38		polymeric precursor method	ferroelectric & piezoelectric devices	[62]
(1-x)BNT-xBKT	151		SSR		[63]
Cooled And Quenched CC-BNT	72.6				[64]
q(1100)-BNT	66				[64]
BKT	125				[64]
0.7BNT-0.2BKT-0.1BLT	216				[64]
BNBK2:1(0.78)	126				[64]
BNBK4:1(0.895)	191				[64]
BNKT-30+La_2O_3 0.2 wt%	155				[64]
0.8 $(Bi_{1/2}Na_{1/2})$ TiO_3-0.2 $(Bi_{1/2}K_{1/2})$ TiO_3 [BNKT-20	157				[64]
BNBT-5.5 (single crystal)	650				[64]
BNBT-5.5 (TGG)	520				[64]
$Bi_{0.5}(Na_{0.70}K_{0.20}Li_{0.10})_{0.5}TiO_3$ (BNKLT)	231		thermal spray process		[65]
$Bi_{12}TiO_{20}$-$Na_{0.5}Bi_{0.5}TiO_3$(BT-NBT)	21.5	500-900	thermal gradient sintering method	Sensors & actuators for industries	[66]
$(Bi_{0.5}Na_{0.5})TiO_3$	109		two-step method	sensors, actuators	[67]
$Na_{0.5}Bi_{4.5}$-$x$$Pr_x$$Ti_4O_{15}$	18 p		SSR		[68]
$0.94Bi_{0.5}Na_{0.5}TiO_3$–$0.06BaTiO_3$	150 -170		SSR		[69]
(1-x) $Bi_{0.5}Na_{0.5}TiO_3$ – x $K_{0.5}Na_{0.5}NbO_3$ + 1 wt. % Gd_2O_3	108		SSR		[70]
$Bi_{1/2}(Na_{0.8}K_{0.2})_{1/2}TiO_3$	148		SSR		[71]

Table 4. Data on NN and its based materials.

NN based materials	d_{33} (pC/N)	T_c (^oC)	Synthesis Method	Applications	Ref.
$NaNbO_3$	28		Molten salt method	Storage memories, energy harvesting, solar energy	[72]
$K_{0.5}Na_{0.5})NbO_3$	80	420			[73]
$(K_{0.465}Na_{0.465}Li_{0.07})NbO_3$	240	460			[73]
$(K_{0.44}Na_{0.52}Li_{0.04})(Nb_{0.84}Ta_{0.1}Sb_{0.06})O$	410	253			[73]
$0.95(K_{0.5}Na_{0.5})NbO_3$-$0.05SrTiO_3$	200	277			[73]
$0.95(K_{0.5}Na_{0.5})NbO_{3}$-$0.05LiTaO_3$	200	430			[73]
$0.94(K_{0.5}Na_{0.5})NbO_3$-$0.06LiNbO_3$	235	460			[73]
$0.95(K_{0.5}Na_{0.5})NbO_3$-$0.05LiSbO_3$	283	392			[73]
$0.7Bi_{0.5}Na_{0.5}TiO_3$-$0.2Bi_{0.5}K_{0.5}TiO_3$-$0.1Bi_{0.5}Li_{0.5}TiO_3$	216	350			[73]
$0.5Na_{0.5}Bi_{0.5}TiO_3$-$0.5K_{0.5}Bi_{0.5}TiO_3$	150	320			[73]
$(Li_{0.05}(Na_{0.51}K_{0.49})_{0.95}(Nb_{0.95}Ta_{0.05})O_3$-$xCe_2O_3$	272		SSR		[74]
$0.963(K_{0.48}Na_{0.52})(Nb_{0.955}Sb_{0.045})O_3$–$0.037(Bi_{0.50}Na_{0.50})HfO_3$	512	238	SSR	ultrasonic transducers, actuators, & sensors	[75]
$(K_{0.4425}Na_{0.52}Li_{0.0375})(Nb_{0.87}Ta_{0.06}Sb_{0.07})O_3$	255		SSR		[76]
$Li_{0.06}(Na_{0.57}K_{0.43})_{0.94}][Ta_{0.05}(Sb_{0.06}Nb_{0.94})_{0.95}]O_3$	306		SSR		[77]
$Na_{0.52}K_{0.44}Li_{0.04})_{1-3x}La_xNb_{0.8}Ta_{0.2}O_3$ (KNLNT-La_x	215	420	SSR		[78]

2.5. Polymer Based Materials (POLX). In general, the piezoelectric polymers will exhibit the piezoelectric nature owing to the molecular structure of the polymers [79]. The d_{33} data of various polymer materials were shown in Table.5. The results were noted to be of order 1-2000 pC/N. From the Table.5, it was clear that the pure organic polymers revealed the moderate piezoelectric coefficient. On the other hand, the same polymers were doped with inorganic piezoelectric elements such as Pb, Na, K, Nb etc., and the obtained d_{33} values were of greater than 1000 pC/N [79]. For instance, the PMN–0.29PT/epoxy (1–3) composite, and PMN0.29PT expressed the huge piezoelectric response by providing the high d_{33} [79]. Therefore, these were used as electromechanical applications.

2.6. Multiferroic Materials (MUFX). In general, the multiferroic materials can exhibit the electrical, piezoelectric, ferroelectric and magnetic behavior. The multiferroic materials as shown in Table.6 showed inverse piezoelectric coefficient ranging from 36 to 400 pm/V [80, 81]. This confirmed us the range of produced strain of different materials for the applied electric field. In the literature, the highest value of inverse d_{33} about 400 pm/V was noted for (0.67-x)$BiFeO_3$-$0.33BaTiO_{3-x}SrZrO_3$ material [81]. It was achieved owing to the presence of tetragonal peaks. Hence, these materials were used for actuators, sensors, information storage and some micro motor systems.

2.7. Glass based materials (GLX).

The Sr-fresnoite ($Sr_2TiSi_2O_8$) + added SiO_2 which is a glass based piezoelectric materials revealed the d_{33} of 10 pC/N [82] (Table.7). This implied that the weak piezoelectric nature was observed in the case of present glass material. This kind of manner may be acquired as a result of the existed less intense polycrystalline phases although it is mixed with silicon dioxide. However, it was suited for high temperature applications.

Fig.5 shows the overall, review analysis of giant d_{33} values of piezoelectric materials. It was also noted that the Pb-based single crystal: (1-x)[$Pb(Mg_{1/3}Nb_{2/3})O_3$]-x[$PbTiO_3$] (PMN-PT) showed the highest value of d_{33} ~ 3500 pC/N. The polymer composite: PMN0.29PT revealed the maximum value of d_{33} ~ 2000 pC/N. In case of BIT based materials, the existed high strains achieved for <001> oriented rhombohedral BNBT-5.5 single crystal exhibited the maximum value of $d_{33}$of 650 pC/N. The BT based composite material: Ba ($Zr_{0.2}Ti_{0.8}$)TO_3-50($Ba_{0.7}Ca_{0.3}$)TiO_3 performed the high piezoelectric coefficient of 620 pC/N. The rest of the materials performed considerable d_{33} values useful for various sensors, transducers, actuators and storage applications.

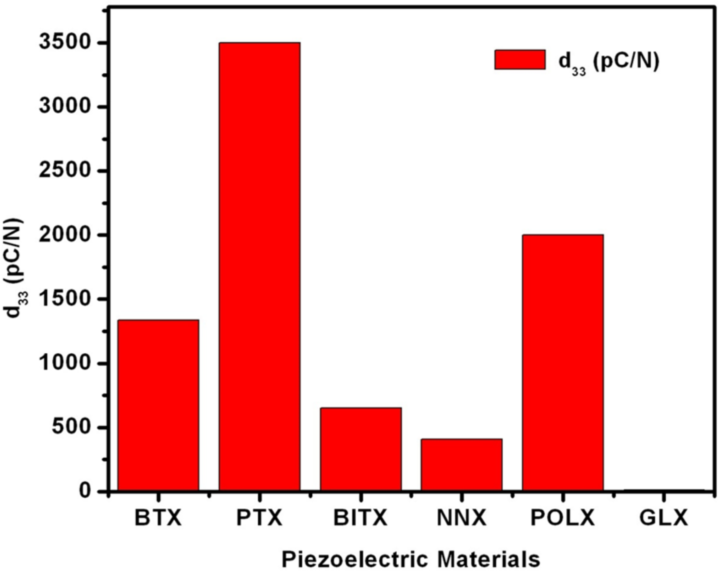

Figure 5. Bar chart for comparing the d_{33} value of different piezoelectric materials.

Table 5. Data on various polymer based materials.

Polymer materials	d_{33} (pC/N)	T_c (^oC)	Synthesis Method	Applications	Ref.
PVDF	13-28			electromechanical transducers	[79]
PVDF–TrFE	24-38				[79]
ParyleneC	2.0				[79]
PI (α-CN) APB/ODPA	5.3-16.5				[79]
Polyimide P150 (β-CN)	16.5				[79]
Polyimide P240 (β CN) APB/ODPA	5.3				[79]
Polyimide (βCN) APB/ODPA	2.5				[79]
Parylene-C	1-2				[79]
ZnO/SU8 nanocomposite	5-8				[79]
PMN–0.29PT/epoxy (1–3) composite	1200				[79]
Cellular polypropylene	200				[79]
Fluorinated and Post treated cellular PP	270				[79]
COC based cellular electrets	13				[79]
Cellular Polyethylene enaphthalate (PEN)	45				[79]
PTFE/FEP multilayer VCP	225				[79]
FEP multilayer	1000				[79]
Cellular PDMS	1148				[79]
Micromachined integrated cellular Parylene	1200				[79]
PZT PIC	500				[79]
PMN0.29PT	2000				[79]

Table 6. Data on multiferroic materials.

Multiferroic materials	Inverse d_{33} (pm/V)	T_c (^oC)	Synthesis Method	Applications	Ref.
$Li_{0.05}Bi_{0.95}Nb_{0.05}Fe_{0.95}O_3$ film,	107.5		sol-gel methods.	actuators and sensors	[80]

Multiferroic materials	Inverse d_{33} (pm/V)	T_c (°C)	Synthesis Method	Applications	Ref.
$Li_{0.025}Bi_{0.975}Nb_{0.025}Fe_{0.975}O_3$ film	62.5		sol-gel methods.		[80]
$BiFeO_3$ film	35.6		sol-gel methods.		[80]
(0.67-x)$BiFeO_3$-0.33$BaTiO_{3-x}SrZrO_3$	400		SSR	informationstorage, sensors, actuators and some micro motor systems	[81]

Table 7. Data on glass based materials.

Glass based materials	d_{33} (pC/N)	T_c (°C)	Synthesis Method	Applications	Ref.
Sr-fresnoite ($Sr_2TiSi_2O_8$) + added SiO_2	10		Standard glass melting techniques	high-temperature applications	[82]

3. CONCLUSIONS

A review of piezoelectric materials with their d_{33} values was performed. As a result of this review, it was concluded that (i) the Pb-based single crystal: (1-x)[$Pb(Mg_{1/3}Nb_{2/3})O_3$]-x[$PbTiO_3$] (PMN-PT) showed the highest value of d_{33} ~ 3500 pC/N. (ii) The polymer composite: PMN0.29PT revealed the maximum value of d_{33} ~ 2000 pC/N. (iii) In case of BIT based materials, the existed high strains achieved for <001> oriented rhombohedral BNBT-5.5 single crystal exhibited the maximum value of d_{33} of 650 pC/N. (iv) The BT based composite material: $Ba(Zr_{0.2}Ti_{0.8})TO_3$-50$(Ba_{0.7}Ca_{0.3})TiO_3$ performed the high piezoelectric coefficient of 620 pC/N. (v) The sodium niobate based material: $(K_{0.44}Na_{0.52}Li_{0.04})(Nb_{0.84}Ta_{0.1}Sb_{0.06})O$ expressed the huge value of d_{33} ~ 410 pC/N. Further the high inverse d_{33} of multiferroic materials was observed for $Li_{0.05}Bi_{0.95}Nb_{0.05}Fe_{0.95}O_3$ film and (0.67-x) $BiFeO_3$-0.33$BaTiO_{3-x}SrZrO_3$. In addition, the d_{33} value of glass material was found and noted to be very small in magnitude (Sr-fresnoite ($Sr_2TiSi_2O_8$) + added SiO_2: 10 pC/N).

4. REFERENCES

1. Holler, F.J.; Skoog, D.A.; Crouch, S.R.*Principles of Instrumental Analysis*, 6th ed.; Cengage Learning. 2007; pp. 9.
2. Kaufmann, P.; Rohring, S.; Supancic, P.; Deluca, M. Influence of ferroelectric domain texture on the performance of multilayer piezoelectric actuators.*J Eur Ceram Soc***2017**, *37*,2039-2046, https://doi.org/10.1016/j.jeurceramsoc.2016.12.029.
3. Bobić,J.D.;Ivanov,M.;Ilić,N.I.;Dzunuzović,A.S.;VijatovićPetrović,M.M.;Banys,J.;Ribic,A.;Despotovic,Z.; Stojanovic, B.D. PZT nickel ferrite and PZT-cobalt ferrite comparative study: structural, dielectric, ferroelectric and magnetic properties of composite ceramics.*Ceramics International***2018**,https://doi.org/10.1016/j.ceramint.2018.01.057.
4. Manotham,S.;Butnoi,P.;Jaita,P.; Kumar, N.;Chokethawai,K.;Rujijangul,G.;Cann,D.P. Large electric field-induced strain and large improvement in energy density of bismuth sodium potassium titanate-based piezoelectric ceramics.*Journal of Alloys and Compounds***2018**, *739*, https://doi.org/10.1016/j.jallcom.2017.12.175.
5. Ehterami, A.; Kazemi, M.; Nazari, B.; Saraeian, P.; Azami, M. Fabrication and characterization of highly porous barium titanate based scaffold coated by Gel/HA nanocomposite with high piezoelectric coefficient for Bone Tissue Engineering Applications.*Journal of the Mechanical Behavior of Biomedical Materials***2017**, *79*, https://doi.org/10.1016/j.jmbbm.2017.12.034.
6. Sharapov, V. *Piezoceramic Sensors, Microtechnology and MEMS*, © Springer-Verlag Berlin Heidelberg 2011; https://doi.org/10.1007/978-3-642-15311-2.
7. Safari, A.; Akdogan, E.K. *Piezoelectric and Acoustic Materials for Transducer Applications*; Springer: New York, 2008.
8. Messing, G.L.; Trolier-McKinstry, S.; Sabolsky, E.M.; Duran,C.; Kwon, S.; Brahmaroutu, B.; Park, P.; Yilmaz, H.; Rehrig, P.W.;Eitel, K.B.; Suvaci, E.; Seabaugh, M.; Oh, K.S. Templated Grain ,Growth of Textured Piezoelectric ceramics. *Crit. Rev. Solid State Mater. Sci.* **2004**, *29*, https://doi.org/10.1080/10408430490490905.
9. Wang, K.; Li, J.F. Domain Engineering of Lead-Free Li-Modified (K,Na)Nbo3 Polycrystals with Highly Enhanced Piezo- electricity. *Adv. Funct. Mater.***2010**, *20*, 1924–1929, https://doi.org/10.1002/adfm.201000284.
10. Gabor, A.S.; Park, J.Y. Concepts, instrument, and model systems that enabled the rapid evolution of surface science.*Surface Science* **2009**, *603*, 1293-1300, https://doi.org/10.1016/j.susc.2008.08.030.
11. Broers, H.; Schattenburg, M.L.; Hector, S.D. Electron beam lithography-Resolution limits.*Microelectronic engineering* **1996**,*32*,143-158.
12. Gao, J.; Xue, D.; Liu, W.; Zhou, C.; Ren, X. Recent Progress on $BaTiO_3$-Based Piezoelectric Ceramics for Actuator Applications.*Actuators***2017**, *6*,https://doi.org/10.3390/act6030024.
13. Sharma,S.; Sharma,A.;Tomar,M.; Puri,N.K.; Gupta, V. NO_x Sensing properties of Barium Titanate thin films.*Procedia Engineering***2014**, *87*, 1067-1070, https://doi.org/10.1016/j.proeng.2014.11.347.
14. Kakimoto, K.I. Fabrication of fibrous $BaTiO_3$-reinforced PVDF composite sheet for transducer application.*Sens. Actuators A: Phys.***2013**, *200*,http://dx.doi.org/10.1016/j.sna.2013.03.007.
15. Wang, F.; Mai, Y.W.; Wang, D.; Ding, R.; Shi, W. High quality barium titanatenanofibers for flexible piezoelectric device applications.*Sensors and Actuators A***2015**, *233*, 195–201, https://doi.org/10.1016/j.sna.2015.07.002.
16. Dong, L.; Stone, D.S.; Lakes, R.S. Enhanced dielectric and piezoelectric properties of x$BaZrO_3$-(12x)$BaTiO_3$ Ceramics.*Journal of Applied Physics* **2012**, *111*, 84107.
17. Shao, S.;Zhang,J.; Zhang,Z.;Zheng,P.; Zhao,M.;Li,J.; Wang, C. High piezoelectric properties and domain configuration in $BaTiO_3$ ceramics obtained through the solid-state reaction route.*J. Phys. D: Appl. Phys.* **2008**,*41*, 125408.
18. Shen, Z.Y.; Li,J.F. Enhancement of piezoelectric constant d 33 in $BaTiO_3$ ceramics due to nano-domain structure.*Journal of the Ceramic Society of Japan***2010**, 118,940-943, https://doi.org/10.2109/jcersj2.118.940.

19. Gao, J.; Xue, D.; Liu, W.; Zhou, C.; Ren, X. Recent Progress on $BaTiO_3$-Based Piezoelectric Ceramics for Actuator Applications.*Actuators***2017**, *6*, 24; https://doi.org/10.3390/act6030024.

20. Shokrollahi, H.; Salimi,F.;Doostmohammadi, A.The fabrication and characterization of barium titanate/akermanitenano-bio-ceramic with a suitable piezoelectric coefficient for bone defect recovery.*Journal of the Mechanical Behavior of Biomedical Materials***2017**, *74*, 365–370, https://doi.org/10.1016/j.jmbbm.2017.06.024.

21. Priya,S.; Sun,N.*Recent advances in piezoelectric and magnetoelectric materials phenomena, Composite Magnetoelectrics*, Chapter: 6, Publisher: Woodhead Publishing, Editors: G Srinivasan, https://doi.org/10.1016/B978-1-78242-254-9.00006-8.

22. Mayamae, J.; Vittayakorn, W.; Sukkha, U.; Bongkarn, T.; Muanghlua, R.; Vittayakorn, N. High piezoelectric response in lead free $0.9BaTiO_3$-(0.1-*x*)$CaTiO_3$-*x*$BaSnO_3$ solid solution.*Ceramic international***2017**, *43*,121-128, https://doi.org/10.1016/j.ceramint.2017.05.252.

23. Zhu, L.F.; Zhang, B.P.; Zhao, L.; Li, J.F. High Piezoelectricity of $BaTiO_3$-$CaTiO_3$-$BaSnO_3$ Lead-Free Ceramics.*Journal of Materials Chemistry C***2014**, *2*, 4764-4771, https://doi.org/10.1039/C4TC00155A.

24. Li, W.; Xu, Z.; Chu, R.; Fu, P.; Zang, G. High piezoelectricd_{33}coefficient of lead-free $(Ba_{0.93}Ca_{0.07})(Ti_{0.95}Zr_{0.05})O_3$ceramics sintered at optimal temperature.*Materials Science and Engineering B***2011**, *176*, 65–67, https://doi.org/10.1016/j.mseb.2010.09.003.

25. Li, W.; Xu, Z.; Chu, R.; Fu, P.; Zang, G. High piezoelectric d_{33} coefficient in $(Ba_{1-x}Ca_x)(Ti_{0.98}Zr_{0.02})O_3$ lead-free ceramics with relative high Curie temperature.*Materials Letters***2010**, *64*, 2325–2327, https://doi.org/10.1016/j.matlet.2010.07.042.

26. Jain, A.; Panwar, A.K.; Jha, A.K. Significant enhancement in structural, dielectric, piezoelectric and ferromagnetic properties of $Ba_{0.9}Sr_{0.1}Zr_{0.1}Ti_{0.9}O_3$-$CoFe_2O_4$ multiferroic composites.*Materials Research Bulletin***2018,** *100*, 367-376, https://doi.org/10.1016/j.materresbull.2017.12.054.

27. Ma, J.; Chen, X.; Lian, H.; Zhang, Q.; Liu, J. Microstructure, dielectric, piezoelectric, and ferroelectric properties of fine-grained $0.94Na_{0.5}Bi_{0.5}TiO_3$-$0.06BaTiO_3$ ceramics. *Journal of the European Ceramic Society***2018**,*39*, https://doi.org/10.1016/j.jeurceramsoc.2018.09.041.

28. Ramovatar, I.C.; Satapathy, S.; Panwar, N. Impact of tin substitution on the structural, dielectric, ferroelectric and piezoelectric properties of $Ba_{0.98}Ca_{0.02}TiO_3$ ceramics.*Physica B; Condensed Matter***2019**, *553*, 68-75, https://doi.org/10.1016/j.physb.2018.10.039.

29. Bai, W.; Wang, L.; Zheng, P.; Wen, F.; Li, L.; Zhai, J.; Ji, Z. Electromechanical response and piezoelectric properties in$(Ba_{0.85}Ca_{0.15})(Zr_{0.1}Ti_{0.9})O_3$piezoceramics using nano-sized AlN modification.*Ceramic International* **2018**, *44*,16040-16050, https://doi.org/10.1016/j.ceramint.2018.06.044.

30. Chen, Z.H.; Li, Z.W.; Qiu, J.H.; Zhao, T.X.; Ding, J.N.; Jia, X.G.; Zhu, W.Q.;Xu, J.J. Y_2O_3 doped $Ba_{0.9}Ca_{0.1}Ti_{0.9}Sn_{0.1}O_3$ ceramics with improved piezoelectric properties.*Journal of the European Ceramic Society***2018**, *38*, 1349-1355, https://doi.org/10.1016/j.jeurceramsoc.2017.10.045.

31. Shin, D.J.; Kim, J.; Koh, J.H. Piezoelectric properties of (1-*x*)BZT-*x*BCT system for energy harvesting applications.*Journals of European Ceramic Society***2018**, *38*, 4395-4403, https://doi.org/10.1016/j.jeurceramsoc.2018.05.022.

32. Yap, E.W.; Glaum, J.; Oddershede, J.; Daniels, J.E. Effect of porosity on the ferroelectric and piezoelectric properties of $(Ba_{0.85}Ca_{0.15})(Zr_{0.1}Ti_{0.9})O_3$ piezoelectric ceramics.*ScriptaMaterialia***2008**, *145*, 122–125, https://doi.org/10.1016/j.scriptamat.2017.10.022.

33. Zhou, M.; Liang, R.; Zhou, Z.; Xu, C.; Nie, X.; Dong, X. Enhanced Curie temperature and piezoelectric properties of $(Ba_{0.85}Ca_{0.15})(Zr_{0.10}Ti_{0.90})O_3$ lead-free ceramics after the addition of $LiTaO_3$.*Materials Research Bulletin* **2018**, *106*,213-219, https://doi.org/10.1016/j.materresbull.2018.05.036.

34. Sharma, S.; Tomar, M.; Puri, N.K.; Gupta, V. Ultraviolet radiation detection by barium titanate thin films grown bysol–gel hydrothermal method.*Sensors and Actuators A***2015**, *230*, 175–181,https://doi.org/10.1016/j.proeng.2014.11.375.

35. Jung, C.H.; Woo, S.I.; Kim, Y.S.; No, K.S. Reproducible resistance switching for $BaTiO_3$ thin films fabricated by RF-magnetron sputtering.*Thin Solid Films***2011**, *519*, 3291–3294, https://doi.org/10.1016/j.tsf.2010.12.149.

36. Tawfik, A.;Hemeda,O.M.;Henaish, A.M.A.;Dorgham, A.M. High piezoelectric properties of modified nanolead titanatezirconat ceramics.*Materials Chemistry and Physics***2018**, *211*, https://doi.org/10.1016/j.matchemphys.2018.01.073.

37. Zhang**,** S.; Li**,** H.; Li**,**M.Size-dependent piezoelectric coefficient d_{33} of $PbTiO_3$ nanoparticles.Materials Letters**2008,** *62*,2438-2440, https://doi.org/10.1016/j.matlet.2007.12.015.

38. Liao, J.H.; Cheng, S.Y.; Wang, H.C.; Wang, C.M. Microstructure and properties of modified $PbTiO_3$ ceramics. *Ferroelectrics***2011**, *127*, 101-106, https://doi.org/10.1080/00150199208223354.

39. Sahul, R. *Effect of Manganese Doping On Pin-Pmn-Pt Single Crystals For High Power Applications*, PhD thesis 2014.

40. Xu, Z.J.; Chu, R.Q.; Li, G.R.; Zeng, H.R.; Yu, H.F.; Yin, Q.R.Strain anisotropy and piezoelectric response along 〈001〉 and 〈110〉 directions in PMN–38PT single crystal.*Materials Letters* **2005**, *59*,1653–1655, https://doi.org/10.1016/j.matlet.2005.01.035.

41. Xu,F.;Chu,F.;Trolier-McKinstry,S.Longitudinal piezoelectric coefficient measurement for bulk ceramics and thin films using pneumatic pressure rig.*J. Appl. Phys.* **1999**, *86*,588; https://doi.org/10.1063/1.370771.

42. Eichhorn, F.; Stenzel, A.;Weisenseel, B.; Travitzky, N.; Kakimoto, K.I.; Greil, P.; Fey, T. Porous piezoelectric ceramics with 3-3-connectivity fabricated by impregnation of cellulose paper structures.*Materials letters***2017**, *206*,158-161, https://doi.org/10.1016/j.matlet.2017.07.007.

43. Taylor, D.V.; Damjanovic, D. Piezoelectric properties of rhombohedral $Pb(Zr,Ti)O_3$$Pb(Zr,Ti)O_3$ thin films with (100), (111), and "random" crystallographic orientation.*Applied Physics Letters***2000**, *76*, 1615,https://doi.org/10.1063/1.126113.

44. .Buurma, A.J.C.;Blake,G.R.;Palstra, T.T.M.; Adem, U.Multiferroic Materials: Physics and Properties.*Reference Module in Materials Science and Materials Engineering***2016**, https://doi.org/10.1016/B978-0-12-803581-8.09245-6.

45. Park, S.E.; Shrout, T.R. Ultrahigh strain and piezoelectric behavior in relaxor based ferroelectric single crystals.*J. Appl. Phys.***1997**, *82*,1804,https://doi.org/10.1063/1.365983.

46. Liu, S.F.;Park,S.E.;Shrout, T.R.;Cross, L.E. Electric field dependence of piezoelectric properties for rhombohedral0.955Pb $(Zn_{1/3}Nb_{2/3})$ $O_3$0.955Pb $(Zn_{1/3}Nb_{2/3})O_3$– 0.045PbTiO$_3$0.045PbTiO$_3$ single crystals.*Journal of Applied Physics***1999**,*85*, 2810, https://doi.org/10.1063/1.369599.
47. Li, S.; Bhalla, A.S.;Newnham, R.E.;Cross, L.E. Quantitative evaluation of extrinsic contribution to piezoelectric coefficient d_{33} in ferroelectric PZT ceramics.*Materials Letters* **1993**, *17*, 21-26, https://doi.org/10.1016/0167-577X(93)90141-J.
48. Lefki,K.;Dormans,G.J.M.Measurement of piezoelectric coefficients of ferroelectric thin films.*J. Appl. Phys.* **1994**, *76*,https://doi.org/10.1063/1.357693.
49. Kuscer, D.; Rojac, T.; Belavič, D.; Zarnik, M.S.;Bradeško, A.; Kos, T.; Malič, B.;Boerrigter, M.; Martin, D.M.;Faccini, M. Integrated piezoelectric vibration system for fouling mitigation in ceramic filtration membranes.*Journal of Membrane Science***2017**, *540*, 277-284, https://doi.org/10.1016/j.memsci.2017.06.054.
50. Khaliq, J.; Deutz, D.B.; Frescas, J.A.C.; Vollenberg, P.; Hoeks, T.; der Zwaag, S.; Groen, P. Effect of the piezoelectric ceramic filler dielectric constant on the piezoelectric properties of PZT-epoxy composites.*Ceramic International***2017**,*43*, 2774-2779, https://doi.org/10.1016/j.ceramint.2016.11.108.
51. Huang, C.; Xu, J.; Fang, Z.; Ai, D.; Zhou, W.; Zhao, L.; Sun, Wang, J.Q. Effect of preparation process on properties of PLZT (9/65/35) transparent ceramics.*Journal of Alloys and Compounds* **2017**, *723*, 602-610, https://doi.org/10.1016/j.jallcom.2017.06.271.
52. Guo, Q.; Cao, G.Z.; Shen, I.Y. Measurements of Piezoelectric Coefficient d_{33} of Lead ZirconateTitanate Thin Films Using a Mini Force Hammer.*Journal of Vibration and Acoustics***2013**, *135*, 11003, https://doi.org/10.1115/1.4006881.
53. Damjanovic, D.; Budimir, M.; Davis, M.; Setter, N.Monodomain versus polydomain piezoelectric response of $0.67Pb(Mg_{1/3}Nb_{2/3})O_3$–$0.33PbTiO_3$ single crystals along nonpolar directions. *Applied Physics Letters***2003**, *83*, 527–529, https://doi.org/10.1063/1.1592880.
54. Algueró,M.;Cheng,B.L.;Guiu,F.;Reece,M.J.;Poole, M.; Alford,N.Degradation of the d_{33} piezoelectric coefficient for PZT ceramics under static and cyclic compressive loading.*Journal of the European Ceramic Society***2001**, *21*,1437-1440, https://doi.org/10.1016/S0955-2219(01)00036-X.
55. Xue, P.; Wu, H.; Lu, Y.; Zhu, X.Recent progress in molten salt synthesis of low-dimensional perovskite oxide nanostructures, structural characterization, properties, and functional applications: A review.*Journal of material science and Technology***2018**, 34, 914-930, https://doi.org/10.1016/j.jmst.2017.10.005.
56. Huo, X.; Zhang, S.; Liu, G.; Zhang, R.; Luo, J. Complete set of elastic, dielectric, and piezoelectric constants of [011]C poled rhombohedral$Pb(In_{0.5}Nb_{0.5})O_3$-$Pb(Mg_{1/3}Nb_{2/3})O_3$-$PbTiO_3$:Mn single crystals.*J. Appl. Phys*.**2013**,*113*, 74106, https://doi.org/10.1063/1.4792661.
57. Yamashita, Y.; Hosono, Y. High Curie temperature piezoelectric single crystals of the $Pb(In_{1/2}Nb_{1/2})O_3$–$Pb(Mg_{1/3}Nb_{2/3})O_3$–$PbTiO_3$ ternary materials system. *Handbook of Advanced Dielectric, Piezoelectric and Ferroelectric Materials* **2008**,https://doi.org/10.1533/9781845694005.1.205.
58. Kalem, V.; Shih, W.Y.; Shih, W.H. Dielectric and piezoelectric properties of PMN-PT ceramics doped with strontium.*Ceramic International***2018**,*44*,2835-2842, https://doi.org/10.1016/j.ceramint.2017.11.029.
59. Luo, X.; Zeng, J.; Shi, X.; Zheng, L.; Zhao, K.; Man, Z.; Li, G.Dielectric, ferroelectric and piezoelectric properties of MnO_2-doped $Pb(Yb_{1/2}Nb_{1/2})O_3$-$Pb(Zr,Ti)O_3$ ceramics.*Ceramic International* **2018**, *44*,8456-8460, https://doi.org/10.1016/j.ceramint.2018.02.042.
60. Yan, Y.; Liu, Z.; Li, Z.; Zhang, M.; Zhang, D.; Feng, Y. Improving piezoelectric properties of Pb(Ni, Nb)O_3-Pb(Hf, Ti)O_3 ceramics by LiF addition.*Ceramic International***2018**, *44*,5790-5793, https://doi.org/10.1016/j.ceramint.2017.12.094.
61. Zhu, R.; Fang, B.; Zhao, X.; Zhang, S.; Chen, Z.; Ding, J.;Luo, H. Enhancing piezoelectric properties of high-Curie temperature PMN-PH-PT piezoelectric ceramics by citrate method.*Journal of Alloys and Compounds***2018**,*735*,496-509, https://doi.org/10.1016/j.jallcom.2017.11.088.
62. Simoes,A.Z.; Cruz,M.P.;Ries,A.; Longo,E.; Varela,J.A.; Ramesh,R. Ferroelectric and piezoelectric properties of bismuth titanate thin films grown on different bottom electrodes by soft chemical solution and microwave annealing.*Materials Research Bulletin***2007**, *42*,975–981, https://doi.org/10.1016/j.materresbull.2006.08.006.
63. Manotham, S.; Butnoi, P.; Jaita, P.; Kumar, N.; Chokethawai, K.; Rujijanagul, G.; Cann, D.P. Large electric field-induced strain and large improvement in energy density of bismuth sodium potassium titanate-based piezoelectric ceramics.*Journal of alloys and compounds***2018**,*739*, 457-467, https://doi.org/10.1016/j.jallcom.2017.12.175.
64. Velev, J.P.;Jaswal,S.S.; Tsymbal, E.Y. Multi-ferroic and magnetoelectric materials and interfaces,Philosophical Transactions: Mathematical.*Physical and Engineering Sciences***2011**, *369*, 3069-3097, https://doi.org/10.1098/rsta.2010.0344.
65. Guo, K.; Mirshekarloo, M.S.; Lin, M.; Yao, K.; Chen, S.; Tay, F.E.H. Microstructure and piezoelectric properties of thermal sprayed $Bi_{0.5}(Na_{0.70}K_{0.20}Li_{0.10})_{0.5}TiO_3$ceramic coatings. *Ceramics International***2018**, https://doi.org/10.1016/j.ceramint.2018.11.016.
66. Yan, S.; Zhao, M.; Wang, C.; Yu, D.; Wang, Y.; Wang, L.; Wang, C. Dielectric and piezoelectric properties of $Bi_{12}TiO_{20-x}Na_{0.5}Bi_{0.5}TiO_3$ polar composite ceramics.*Journal of Alloys and Compounds***2019**, *774*, 471–476, https://doi.org/10.1016/j.jallcom.2018.10.054.
67. Bai, W.; Wang, L.; Zheng, P.; Wen, F.; Li, lili, Ji, Z., &Zhai, J. Enhanced thermal stability, hardening of piezoelectric property, and mediated electromechanical response in $(Bi_{0.5}Na_{0.5})TiO_3$-based piezoceramics via composite approach. *Ceramics International***2018**, *44*, 17022–17032, https://doi.org/10.1016/j.ceramint.2018.06.145.
68. Chen, Y.; Zhang, C.C.; Qin, L.; Jiang, C.B.; Liu, K.H.; Ma, C.; Wu, Z.T.; Pan, R.K.; Cao, W.Q.; Ye, C.; Li, Z. Enhanced dielectric and piezoelectric properties in $Na_{0.5}Bi_{4.5}Ti_4O_{15}$ ceramics with Pr-doping.*Ceramics International***2018**, *44*,https://doi.org/10.1016/j.ceramint.2018.07.037.
69. Han, W.H.; Koh, J.H. Shrinkage mechanism and enhanced piezoelectric properties of Ta doped $0.94Bi_{0.5}Na_{0.5}TiO_3$–$0.06BaTiO_3$ lead free ceramics.*Ceramic International***2018**,*44*,5352-5358, https://doi.org/10.1016/j.ceramint.2017.12.155.
70. Pattipaka, S.; James, A.R.; Dobbidi, P. Enhanced dielectric and piezoelectric properties of BNT-KNNG piezoelectric ceramics. *Journal of Alloys and Compounds***2018**, *765*, 1195–1208, https://doi.org/10.1016/j.jallcom.2018.06.138.
71. Zhang, H.; Zhou, J.; Shen, J.; Yang, X.; Wu, C.; Han, K.; Zhao, Z.; Chen, W. Enhanced piezoelectric property and

promoted depolarization temperature in Fe doped $Bi_{1/2}(Na_{0.8}K_{0.2})_{1/2}TiO_3$ lead-free ceramics. *Ceramics International* **2017**, *43*, 16395–16402, https://doi.org/10.1016/j.ceramint.2017.09.015.

72. Xue, P.; Wu, H.; Lu, Y.; Zhu, X. Recent progress in molten salt synthesis of low-dimensional perovskite oxide nanostructures, structural characterization, properties, and functional applications: A review. *Journal of material science and Technology* **2018**, *34*, 914-930, https://doi.org/10.1016/j.jmst.2017.10.005.

73. Marquis, B.T.; Vetelino, J.F. A semiconducting metal oxide sensor array for the detection of NO_x and NH_3 *Sens. Act. B* **2001**, *77*, 100-110

74. Huang, R.; Zhao, Y.; Yan, D. The enhanced piezoelectric property of $(Li,K,Na)(Nb,Ta)O_3$ lead-free ceramics induced by rare earth oxide doping. *Journal of Alloys and Compounds* **2018**, *750*, 124-129, https://doi.org/10.1016/j.jallcom.2018.03.370.

75. Liu, D.; Zhang, X.; Su, W.; Wang, X.; Yao, W.; Zhou, C.; Zhang, J. Outstanding piezoelectric properties, phase transitions and domain configurations of $0.963(K_{0.48}Na_{0.52})(Nb_{0.955}Sb_{0.045})O_3{-}0.037(Bi_{0.50}Na_{0.50})HfO_3$ ceramics. *Journal of Alloys and Compounds* **2018**, *779*, https://doi.org/10.1016/j.jallcom.2018.11.183.

76. Dong, Z.J.; Pu, Y.P.; Liu, Y.W. Influence of $Bi_4Ti_3O_{12}$ doping on structural and piezoelectric properties of $(K_{0.4425}Na_{0.52}Li_{0.0375})(Nb_{0.87}Ta_{0.06}Sb_{0.07})O_3$ lead-free ceramics. *Ceramics International* **2017**, *43*, 55–58, https://doi.org/10.1016/j.ceramint.2017.05.210.

77. Xu, F.; Chen, J.; Lu, Y.; Zhang, Q.; Zhang, Q.; Zhou, T.; He, Y. Exploration on the origin of enhanced piezoelectric properties in transition-metal ion doped KNN based lead-free ceramics. *Ceramics International* **2018**, *44*, 16745–16750. https://doi.org/10.1016/j.ceramint.2018.06.104.

78. Yang, W.; Wang, L.; Li, H.; Han, J.; Xiu, H.; Zhou, Z. Piezoelectric properties and diffusion phase transition around PPT of La-doped $(Na_{0.52}K_{0.44}Li_{0.04})$ $Nb_{0.8}Ta_{0.2}O_3$ lead-free piezoelectric ceramics. *Physica B: Condensed Matter* **2016**, *498*, 59–64, https://doi.org/10.1016/j.physb.2016.06.022.

79. Khaled, S.; Sameoto, R.D.; Evoy, S. A review of piezoelectric polymers as functional materials for electromechanical transducers. *Smart Mater. Struct*. **2014**, *23*, 33001, 26.

80. Hou, Y.; Han, R.; Liu, Y.; Luo, L.; Li, W.; Fei, W. Enhanced piezoelectric properties in $Li_xBi_{1-x}NbFe_{1-x}O_3$ films contributed by low-symmetry phase and self-polarization. *Ceramics International* **2018**, *45*, 3723-3728, https://doi.org/10.1016/j.ceramint.2018.11.037.

81. Zhao, N.; Fan, H.; Ren, X.; Ma, J.; Bao, J.; Guo, Y.; Zhou, Y. Dielectric, conductivity and piezoelectric properties in $(0.67\text{-}x)BiFeO_3\text{-}0.33BaTiO_3\text{-}xSrZrO_3$ ceramics. *Ceramics International* **2018**, *44*, https://doi.org/10.1016/j.ceramint.2018.07.116.

82. Mark, J.; Vullo, D.P.; Kocher, M.; Hovhannisyan, M.; Letz, M. Piezoelectric glass-ceramic for high-temperature applications. *Journal of Non-Crystalline Solids* **2018**, *501*, 159-166, https://doi.org/10.1016/j.jnoncrysol.2018.03.038.

5. ACKNOWLEDGEMENTS

The authors express thankful to N. Suresh Kumar for providing the literature on the present work and sharing the ideas with us. Dr. D. Baba Basha is also thankful to Majmaah University Al'Majmaah, K.S.A, for their encouragement towards research work.